THE ASTROPHYSICAL JOURNAL, 271:744–753, 1983 August 15

THE LIGHT CURVE OF THE ZZ CETI STAR G226–29

S. O. KEPLER,[1] E. L. ROBINSON, AND R. E. NATHER
McDonald Observatory and Department of Astronomy, The University of Texas at Austin
Received 1982 November 11; accepted 1983 February 4

ABSTRACT

G226–29 is a pulsating DA white dwarf, or ZZ Ceti star. Using 65 hr of high-speed photometry accumulated from 1980 to 1982, we have decomposed the light curve of G226–29 into its component pulsations. There are three pulsations in the light curve, all of which have periods close to 109.3 s. Their fractional semiamplitudes and periods are 0.0031 and 109.08684 s, 0.0011 and 109.27929 s, and 0.0031 and 109.47242 s. The pulsations are evenly spaced in frequency, and those with the longest and shortest periods have nearly equal amplitudes. We propose that the pulsations are *g*-mode pulsations with the same values of l and k, but with different values of m, whose periods have been split by slow rotation of the white dwarf. Depending on the specific value of l we assign to the pulsations, the equatorial rotational velocity of G226–29 is between 1 and 2 km s^{-1}.

Subject headings: stars: individual — stars: pulsation — stars: rotation — stars: white dwarfs

I. INTRODUCTION

The ZZ Ceti stars are pulsating DA white dwarfs lying within an instability strip a few thousand degrees wide centered near $T_e = 11{,}200$ K (Greenstein 1982). Their pulsations have typical periods between 100 and 1200 s and typical amplitudes between 0.003 and 0.30 mag (Robinson 1979). They are always multiperiodic. Several theoretical studies have shown that *g*-mode nonradial pulsations have periods similar to the observed periods of the ZZ Ceti stars, and that *g*-modes are pulsationally unstable in models of DA white dwarfs with temperatures near 11,200 K (Winget 1981; Dolez and Vauclair 1982; Winget *et al.* 1982). Consequently, it is universally accepted that most, and perhaps all, of the pulsations of the ZZ Ceti stars are *g*-mode pulsations.

The pulsations of the ZZ Ceti stars are powerful tools for investigating the structure and evolution of single white dwarfs. Specifically, the properties of the pulsations depend strongly on the onionskin composition layers of the white dwarfs and can be used to measure many of the properties of the layers, including their masses and the sharpness of the transition zones between them. These measurements will help to clarify such issues as what role accretion from the interstellar medium is playing in determining the composition of the white dwarf atmospheres and how important convective mixing and diffusion are in determining the structure of the white dwarf envelope. In addition, the rate of change of the *g*-mode pulsation periods can be used to measure the cooling rate of a white dwarf. The cooling rate can then be used to derive the core composition of the white dwarf, and to derive white dwarf birth rates from the observed white dwarf luminosity function. To use the pulsations in this way, we must first measure their periods and amplitudes. Unfortunately, measuring these quantities is a difficult task because the light curves of the ZZ Ceti stars are extremely complex. Four or more pulsations have been found in every ZZ Ceti star, and in many of the stars the amplitudes and periods of the pulsations change on time scales as short as a few hours. As a result, only three of the 17 known ZZ Ceti stars have had their light curves analyzed completely: R548 by Stover *et al.* (1980), L19–2 by O'Donoghue (1981), and G117–B15A by Kepler *et al.* (1982).

In this paper we report our analysis of the light curve of one more ZZ Ceti star, the proper motion star G226–29 (Giclas, Burnham, and Thomas 1971). The variability of G226–29 was first discovered by J. T. McGraw and G. Fontaine (1982, private communication), who found a period of 109.3 s and an amplitude of 0.006 mag for the variations. McGraw and Fontaine also recognized that the 109.3 s variation must be an unresolved combination of pulsations, but their data were not extensive enough for them to determine the individual pulsation periods or to develop an ephemeris for the light curve. We have observed G226–29 on 30 nights in the last 2 years and have used this large data base to reanalyze the star's light curve. Using these data, we derive an exact ephemeris for the light curve, we show that the variation at 109.3 s is composed of three pulsations, and we find the periods and amplitudes of the individual components.

[1]Fellow of the Conselho Nacional de Desenvolvimento Cientifico e Tecnologico (CNPq) and the Instituto de Fisica da Universidade Federal do Rio Grande do Sul, Brazil.

TABLE 1

OBSERVATIONS OF G226–29

Run	Start Time (UT)		Length (hr)	Integration Time (s)	Telescope (m)
MG67 ...	80 Apr 8	09:35	1.7	5	0.9
MG70 ...	80 Apr 9	09:41	1.7	5	0.9
MG73 ...	80 Apr 10	10:03	1.3	5	0.9
MG76 ...	80 Apr 11	10:11	1.1	5	0.9
2518.....	80 Jun 14	03:49	5.2	5	2.1
2527.....	80 Jun 18	04:19	2.2	4	2.1
2533.....	80 Jul 10	03:31	5.0	5	2.1
2535.....	80 Jul 11	03:33	1.9	5	2.1
2537.....	80 Jul 12	03:34	0.3	5	2.1
2540.....	80 Jul 14	03:39	1.4	5	2.1
2543.....	80 Sep 6	04:32	1.4	5	2.1
2549.....	80 Sep 8	03:15	0.8	5	2.1
2551.....	80 Sep 12	04:27	0.5	5	2.1
2554.....	80 Oct 4	02:39	1.3	5	0.9
2557.....	80 Oct 5	01:58	1.8	5	0.9
2591.....	81 Jan 31	10:35	1.8	3	2.1
2595.....	81 Feb 2	10:39	1.7	3	2.1
2596.....	81 Feb 5	10:31	1.9	3	2.1
2598.....	81 Feb 6	10:59	1.3	5	2.1
2602.....	81 Mar 31	07:51	2.3	5	0.9
2605.....	81 Apr 1	08:41	2.7	5	0.9
2607.....	81 Apr 4	06:57	2.0	5	0.9
2610.....	81 Apr 9	07:06	4.2	5	0.8
2612.....	81 May 5	06:00	4.7	5	0.9
2614.....	81 May 8	05:57	2.0	5	0.9
2616.....	81 May 9	05:58	4.4	5	0.9
2657.....	82 Mar 26	09:54	1.7	5	2.1
2659.....	82 Mar 28	08:10	1.4	5	2.1
2660.....	82 Apr 25	04:00	7.0	5	0.9
2662.....	82 Apr 26	04:13	1.2	6	0.9

II. OBSERVATIONS

Our data consist of light curves of G226–29 obtained with a high-speed, two-channel photometer (Nather 1973) on the 2.1, 0.9, and 0.8 m telescopes at McDonald Observatory. The observations were made without filters using a blue-sensitive photomultiplier tube (an RCA 8850). The time base is UTC broadcast by WWV, which we convert to heliocentric Julian ephemeris date by our usual method (Kepler *et al.* 1982). This time base is accurate to better than 0.5 s, with the errors resulting primarily from inaccuracies in the heliocentric correction. We accumulated a total of 65 hr of photometry, the details of which are given in Table 1. A portion of the light curve of G226–29 on the night of 1980 July 10 is shown in Figure 1.

III. ANALYSIS OF THE LIGHT CURVE

a) *The Individual Nights*

We first calculated power spectra of the individual light curves of G226–29 (see Kepler *et al.* 1982 for a description of our method for calculating the power spectra). The light curves are generally too short to resolve the triplet of pulsations at 109.3 s, so most of the power spectra show only a single peak at that period. The semiamplitude of the peak varies from 0.1% to 0.7% from night to night. When its amplitude is low, the 109.3 s variation is difficult to detect in the power spectra of the shorter light curves, which could explain why the pulsations of G226–29 were not detected during a previous survey for variable white dwarfs (McGraw 1976). The power spectra of the longest runs, those longer than 4.5 hr, partially resolve the peak at 109.3 s into its components. Two components are visible in the power spectrum of our longest light curve, shown in Figure 2. Although the power spectra of these longer light curves suffice to show that there is more than one component to the 109.3 s variation, the detailed properties of the individual components cannot be measured from the power spectra because the resolution of the power spectra is too poor. Neither the amplitudes nor the periods nor even the number of the components are given correctly because the components lie within the side lobes of each other's spectral windows.

Since the 109.3 s variation is unresolved or underresolved in our data (that is, it is acting like a single sine curve), we can measure its mean period for each night.

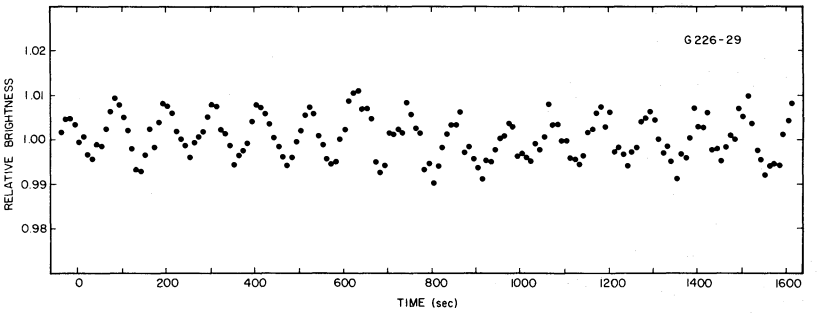

FIG. 1.—A portion of the light curve of G226–29 in unfiltered light on 1980 July 10. The light curve has been normalized so that the time-averaged brightness is equal to 1.00.

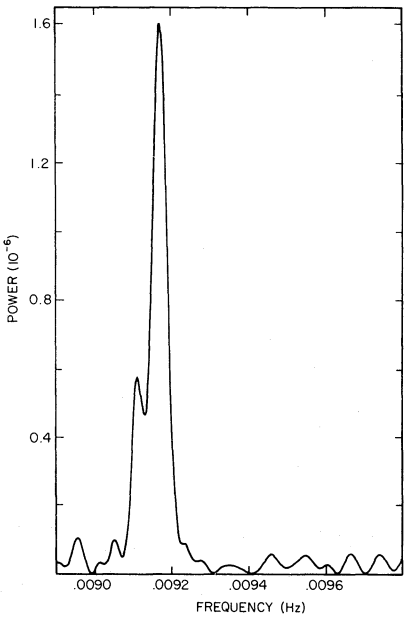

FIG. 2.—The low-frequency portion of the power spectrum of the light curve of G226–29 during run 2660. The 109.3 s variation is partially resolved into its components in this power spectrum.

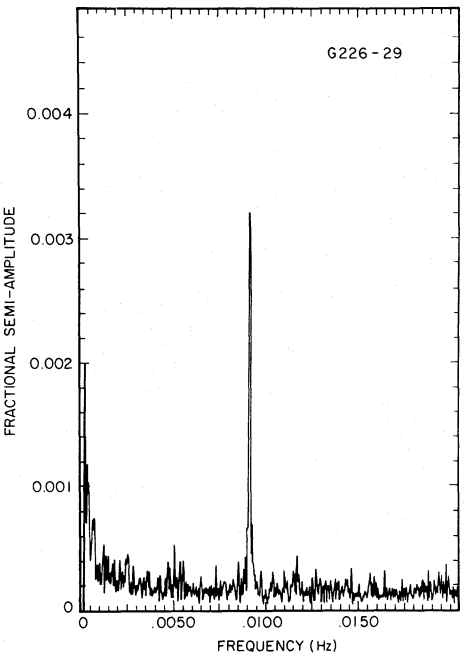

FIG. 3.—The low-frequency portion of the amplitude spectrum of the light curve of G226–29. This spectrum is the average of the amplitude spectra of three of our longest light curves.

We have done so by fitting sine curves to each of the light curves by nonlinear least squares and solving for the best period. The mean period was the same on all nights to within the measurement errors; a weighted average of the mean periods from the individual nights yielded 109.29 ± 0.03 s. The formal error on the weighted average period is larger than might be expected, because the phase shifts associated with beating between the components of the 109.3 s variation mimic small period changes and increase the scatter in the periods from the individual nights. If only a few nights were included in the weighted average period, these nonrandom phase shifts could also bias the average. For our average, however, the bias is negligible because we have included data from 30 independent nights.

In order to search for pulsations other than those at 109.3 s, we calculated an average amplitude spectrum of G226–29 by averaging the amplitude spectra of our three longest light curves. A portion of the average amplitude spectrum is shown in Figure 3. There are no peaks with semiamplitudes larger than twice the standard deviation of 0.0004. The first harmonic of the 109.3 s variation has a fractional semiamplitude less than 0.00011. To be complete, we note that there are also a few peaks at periods longer than 2000 s with fractional semiamplitudes near 0.002. We suspect these long period

TABLE 2

AMPLITUDE AND PHASE OF THE 109 s PULSATION OF G226−29

Original Run Number	Length of Light Curve Section (hr)	HJED at a Maximum (2,440,000.0+)	Timing Error (s)	Fractional Semiamplitude	Amplitude Error
MG67	0.82	4337.900909	1.2	0.0057	0.0004
	0.82	4337.936296	1.4	0.0051	0.0004
MG70	0.81	4338.906937	1.1	0.0061	0.0003
	0.82	4338.941109	1.0	0.0063	0.0003
MG73	1.36	4339.920770	1.1	0.0055	0.0003
MG76	1.10	4340.926707	13.6	0.0023	0.0004
2518	0.83	4404.661221	1.5	0.0023	0.0002
	0.83	4404.695521	2.6	0.0012	0.0002
	0.83	4404.729916	1.3	0.0022	0.0001
	0.83	4404.765376	0.8	0.0040	0.0002
	0.83	4404.799563	0.6	0.0052	0.0002
	0.83	4404.834968	0.5	0.0059	0.0002
2527	2.23	4408.681994	0.7	0.0031	0.0001
2533	0.83	4430.649670	0.5	0.0060	0.0002
	0.83	4430.683832	0.5	0.0063	0.0002
	0.83	4430.718008	0.5	0.0061	0.0002
	0.83	4430.753420	0.7	0.0058	0.0002
	0.83	4430.787552	0.8	0.0045	0.0002
	0.81	4430.822312	1.8	0.0030	0.0003
2535	0.83	4431.649607	1.0	0.0029	0.0001
	0.83	4431.683745	0.8	0.0041	0.0002
2537	0.29	4432.650149	2.7	0.0017	0.0002
2540	1.36	4434.653506	0.7	0.0057	0.0002
2543	1.42	4488.689139	1.1	0.0055	0.0003
2549	0.79	4490.636397	0.8	0.0046	0.0002
2551	0.52	4494.685509	6.3	0.0013	0.0004
2554	1.33	4516.611003	1.5	0.0033	0.0003
2557	1.78	4517.582347	1.8	0.0025	0.0002
2591	1:80	4635.942583	2.3	0.0014	0.0002
2595	1.69	4637.945169	0.4	0.0056	0.0001
2596	0.33	4640.940192	2.0	0.0020	0.0002
	0.33	4640.954085	2.9	0.0013	0.0002
	0.32	4640.967826	2.8	0.0012	0.0002
	0.33	4640.981629	2.7	0.0014	0.0002
	0.33	4640.995457	2.2	0.0016	0.0002
2598	0.30	4641.959122	1.5	0.0041	0.0003
	0.33	4641.973028	2.5	0.0023	0.0003
	0.25	4641.986996	3.3	0.0025	0.0004
	0.32	4642.000945	3.2	0.0016	0.0003
2602	0.53	4694.829288	1.9	0.0037	0.0004
	0.56	4695.852077	1.4	0.0049	0.0004
	0.53	4694.874815	1.4	0.0057	0.0004
	0.56	4694.898840	1.4	0.0056	0.0004
2605	0.56	4695.864463	1.9	0.0041	0.0004
	0.56	4695.887204	1.4	0.0050	0.0004
	0.54	4695.909983	1.1	0.0062	0.0003
	0.53	4695.934024	1.0	0.0066	0.0004
	0.54	4695.956797	0.9	0.0076	0.0003
2607	0.56	4698.792512	1.5	0.0062	0.0005
	0.56	4698.815269	1.3	0.0065	0.0004
	0.54	4698.839283	1.0	0.0080	0.0004
2610	0.56	4703.798607	1.5	0.0055	0.0004
	0.56	4703.822635	1.1	0.0065	0.0004
	0.54	4703.845387	1.0	0.0073	0.0004
	0.56	4703.868164	1.0	0.0073	0.0004
	0.53	4703.892194	1.2	0.0064	0.0004
	0.56	4703.914969	1.1	0.0060	0.0003
	0.53	4703.937729	1.3	0.0058	0.0004
2612	0.55	4729.752388	1.3	0.0056	0.0004
	0.56	4729.775197	1.5	0.0044	0.0003
	0.56	4729.799212	1.8	0.0042	0.0004

TABLE 2—*Continued*

Original Run Number	Length of Light Curve Section (hr)	HJED at a Maximum (2,440,000.0+)	Timing Error (s)	Fractional Semiamplitude	Amplitude Error
	0.53	4729.821987	4.2	0.0017	0.0004
	0.56	4729.844638	4.0	0.0020	0.0004
	0.53	4729.868458	9.4	0.0008	0.0004
	0.54	4729.891078	3.4	0.0021	0.0004
	0.56	4729.913795	2.4	0.0027	0.0003
2614	0.56	4732.749604	5.9	0.0013	0.0004
	0.54	4732.773497	3.2	0.0024	0.0004
	0.54	4732.796262	1.9	0.0039	0.0004
2616	0.56	4733.751198	3.5	0.0023	0.0004
	0.56	4733.774243	11.7	0.0007	0.0004
	0.54	4733.796955	7.5	0.0010	0.0004
	0.56	4733.821255	3.9	0.0017	0.0003
	0.55	4733.843961	2.5	0.0031	0.0004
	0.54	4733.866861	2.1	0.0044	0.0005
	0.56	4733.889603	1.7	0.0054	0.0005
2657	1.71	5053.908213	3.0	0.0009	0.0001
2659	1.38	5056.842273	1.0	0.0028	0.0002
2660	1.16	5084.669730	4.6	0.0033	0.0008
	1.16	5084.717765	8.3	0.0017	0.0007
	1.16	5084.768055	4.9	0.0018	0.0004
	1.11	5084.817275	2.3	0.0035	0.0004
	1.10	5084.866540	1.8	0.0053	0.0005
	1.17	5084.914621	3.6	0.0056	0.0010
2662	1.04	5085.677331	2.9	0.0044	0.0007

variations are real because they were often present when the quality of the night was excellent, and they were absent from the light curves of the comparison stars observed simultaneously with the second channel of the photometer. Nevertheless, we cannot establish the existence of the long-period variations conclusively because our data do not permit precise removal of slow extinction changes that could introduce spurious variations similar to those observed.

b) The Period of the Amplitude Modulation

A straightforward attempt to derive the ephemeris of the 109.3 s variation by calculating the power spectrum of data from several nights simultaneously produced inconsistent and contradictory results. An attempt to fit a single sine curve to data from several nights simultaneously fared no better. Therefore, to study the behavior of the amplitude and phase of the 109.3 s variation in more detail, we partitioned the light curves into 85 nonoverlapping segments roughly 40 minutes long. We measured the amplitude and time of maximum of the 109.3 s variation during each segment by fitting the segments with a sine curve with a period of 109.29 s. The resulting fractional semiamplitudes and times of maximum are given in Table 2.

The amplitudes in Table 2 cycle smoothly from 0.001 to 0.007, but the period cannot be determined unambiguously from the amplitude data alone. If the amplitude goes through one maximum per beat cycle, the beat period is 8.6 hr; if the amplitude goes through two maxima per cycle, the period is 17.2 hr. The amplitudes are different at the two maxima of the 17.2 hr period, suggesting that the 17.2 hr period is correct, but not different enough to prove it is correct. Fortunately, the timing data in Table 2 eliminated the 8.6 hr period. Each time the amplitude goes to a minimum, the phase of the 109.3 s variation increases or decreases by 155°, so that alternate amplitude maxima can be distinguished by their different phases. The 17.2 hr beat period is therefore the correct one.

We optimized the 17.2 hr period using a period finding technique devised by Deeming (Bopp *et al.* 1970). In this technique, the amplitude data are "folded" at trial periods to form a plot of the measured amplitudes as a function of phase in the trial period. The best period is the one that minimizes the scatter between successive data points in the plot. The periodogram for the amplitude data is shown in Figure 4, where the quantity Q measures the scatter and is plotted against trial period. The best period, given by the minimum Q, is 17.2068 ± 0.0005 hr; all other periods, including the various aliases of 17.2068 hr, can be eliminated. The plot of the amplitude as a function of phase in the 17.2068 hr modulation period is shown in Figure 5.

c) The Average Pulsation Period

We can now understand why the straightforward attempts to fit sine curves to data from more than one

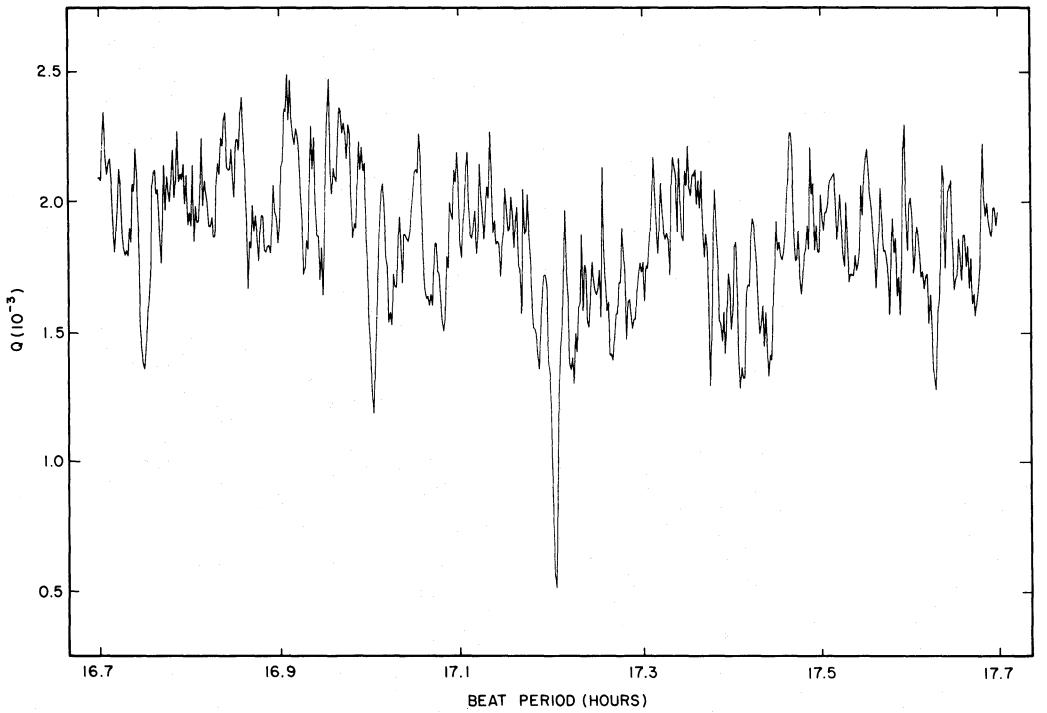

FIG. 4.—The periodogram of the amplitudes of the 109.3 s variation given in Table 2. The quantity Q measures the scatter in the folded amplitude curve at each trial period in the periodogram. The minimum value for Q corresponds to the minimum scatter, and gives the best period for the amplitude variation.

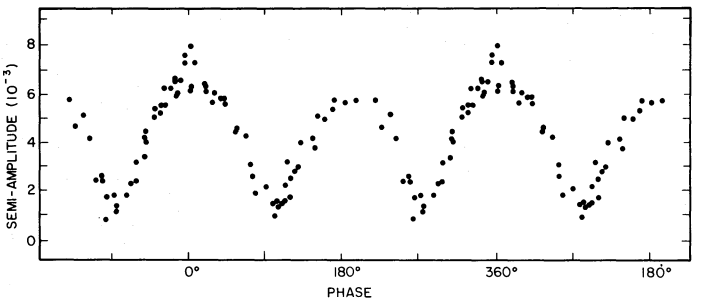

FIG. 5.—This figure shows the amplitudes of the 109.3 s variation, given in Table 2, folded at the beat period of 17.2068 hr

night gave contradictory results. Data obtained on two successive nights will be separated by about 24 hr, which is about 1.5 cycles of the 17.2 hr period. Because the phase of the 109.3 s variation shifts by 155° in alternate amplitude maxima, data from successive nights will usually be shifted by 155° in phase. However, it is possible for measurements made 24 hr apart to sample the 17.2 hr cycle in such a way that the 109.3 s variation remains in phase. This will happen on average about once every four or five pairs of nights. Thus, most 24 hr intervals will require a pulsation period giving a 155° phase shift after 24 hr, but a few 24 hr intervals will require a pulsation period giving a 0° phase shift after 24 hr. Data from three or more successive nights can require both pulsation periods, causing great difficulties for power spectra and least squares methods.

To derive the correct period of the 109.3 s variation, it is necessary to account explicitly for the effects of the 155° phase shifts. To do this, we added 155° (= 47 s) to the times of maxima in Table 2 if the time of maximum fell into the second half of the amplitude modulation cycle, and then we used the corrected times of maxima to recalculate the mean periods for each night. The weighted average of these revised periods for the individual nights yielded 109.29 ± 0.01 s. This period is the same as the period we derived in § III*a*, but its standard

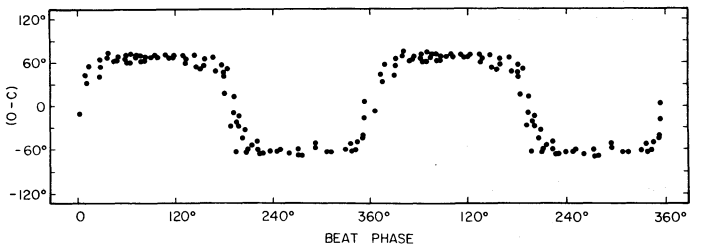

FIG. 6.—The $(O-C)$ diagram for the maxima of the 109.3 s variation given in Table 2. Each dot is the difference between an observed time of maximum and the time of maximum predicted by a linear ephemeris with a period of 109.27929 s. The data have been folded at the beat period of 17.2068 hr.

deviation is 3 times smaller because we have eliminated the scatter in the timings introduced by the 155° phase shifts.

The weighted average period is accurate enough to join timings from successive nights without any ambiguity in the cycle count. Therefore, using timings from pairs of successive nights we could improve the period, and with the improved period we could join timings separated by several nights. With further improvement in the period we could join timings separated by 1 month without any error in the cycle count. Since G226–29 has a declination of 59°, we can observe it for 10 months each year from McDonald Observatory, so that we did not have to bridge gaps longer than a few months.

Armed with unique cycle counts, E, and a reasonably accurate period, we fit the following linear ephemeris by least squares to the corrected timings, t_{max}:

$$t_{max} = t_0 + PE. \quad (1)$$

The optimum values of t_0, an initial time of maximum, and P, the period of the 109.3 s variation, are

$$t_0 = \text{HJED } 2{,}444{,}337.90116 \pm 0.00004,$$

$$P = 109.27929 \pm 0.00002 \text{ s}.$$

As a final check of our analysis, we calculated the $(O-C)$ diagram for the *uncorrected* timings, where O is the observed time of maximum given in Table 2, and C is the expected time calculated from equation (1). We then folded the $(O-C)$ diagram at the 17.2068 hr period of the phase modulation to show the form of the 155° phase shifts explicitly. The resulting phase diagram is displayed in Figure 6. The phase diagram has the form of a slope-shouldered square wave, and, as expected, the timings in the second half of the 17.2068 hr cycle are retarded by 155°. The square wave is not symmetrical. The positive part of the square wave lasts 16% longer than the negative part. The same 16% asymmetry can be found, after the fact, in the amplitude curve shown in Figure 5.

d) Interpretation as Three Beating Pulsations

The perfect regularity of the 17.2068 hr amplitude and phase modulation shows that the 109.3 s variation can be decomposed into two or more pulsations with constant amplitude and phase, but the exact form of the modulation immediately eliminates the simple models in which the 109.3 s variation is the sum of just two beating pulsations. Two pulsations beating together cannot produce a double-peaked amplitude diagram with unequal amplitudes in the two peaks, they cannot produce the slope-shouldered square wave with a 155° phase shift, and they cannot produce an asymmetric square wave in a phase diagram. Three pulsations equally spaced in frequency are necessary to fit the observations. The 17.2068 hr beat period of the double-peaked amplitude modulation and the average period of the 109.3 s variation determine the periods of the three pulsations uniquely:

$$P_0 = 109.27929 \text{ s},$$

$$P_1 = 109.08684 \text{ s},$$

$$P_2 = 109.47242 \text{ s}.$$

We simultaneously fit three sine curves with these periods to our *original* light curves to derive the best amplitudes and phases for the pulsations. The results are:

$$A_0 = 0.00117 \pm 0.00004,$$

$$T^0_{max} = 4337.901243 \pm 0.000008,$$

$$A_1 = 0.00305 \pm 0.00004,$$

$$T^1_{max} = 4337.902060 \pm 0.000003,$$

$$A_2 = 0.00317 \pm 0.00004,$$

and

$$T^2_{max} = 4337.902144 \pm 0.000003,$$

where $T^i_{max} + 2{,}440{,}000$ is the heliocentric Julian ephemeris date of maximum light of pulsation i. The

standard deviations of the amplitudes are the formal standard deviations calculated by the least squares program. They can be used when intercomparing the amplitudes of the pulsations, but the true errors are larger because of systematic errors in the corrections for extinction and sky background.

The amplitudes of pulsations 1 and 2 differ by less than two standard deviations. Therefore, the triplet of pulsations consists of two side pulsations with nearly equal amplitudes, and a central pulsation with a lower amplitude. We can show that this model accounts completely for the amplitude and phase modulations of the 109.3 s variation as follows. The intensity variations caused by the triplet of pulsations have the form:

$$I(t) = A_0 \sin(w_0 t + \phi_0) + A_1 \cos(w_0 + \Delta w)t + A_1 \cos(w_0 - \Delta w)t, \quad (2)$$

where we have forced the side pulsations to have the same amplitude, and we have defined t to be zero when the two side pulsations are in phase. Equation (2) can be written as

$$I(t) = A(t) \sin[w_0 t + \phi(t)], \quad (3)$$

where the amplitudes and phases in equation (3) are given by

$$A^2(t) = A_0^2 + 4A_0A_1 \sin\phi_0 \cos\Delta wt + 4A_1^2 \cos^2 \Delta wt \quad (4)$$

and

$$\tan\phi(t) = \tan\phi_0 + 2A_1(A_0 \cos\phi_0)^{-1} \cos\Delta wt. \quad (5)$$

The parameters of equations (4) and (5) are fixed by the results of the least squares fit and are

$$P_0 = 109.27929 \text{ s}, \quad A_0 = 0.0012,$$

$$\Delta w = 1.01433 \times 10^{-4} \text{ rad s}^{-1},$$

$$A_1 = 0.0031, \quad \text{and} \quad \phi_0 = 35°.$$

The amplitude and phase modulations given by equations (4) and (5) have been plotted with the observed amplitudes and phases in Figures 7 and 8. The equations fit the data to within the measurement errors. As there are no systematic differences between the data and the curves, the model accounts completely for the behavior of the 109.3 s variation; if there are other components in the variation, the sum of their fractional semiamplitudes must be less than 0.0005.

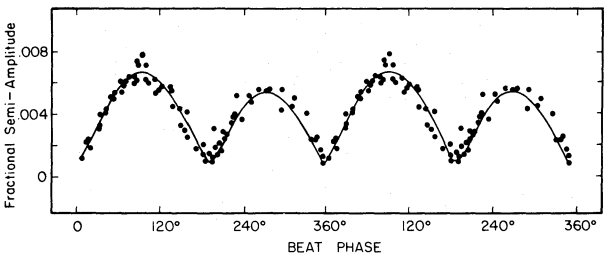

FIG. 7.—The dots are the observed amplitudes of the 109.3 s variation given in Table 2. They have been folded at the beat period of 17.2068 hr. The solid line is a plot of eq. (4) with semiamplitudes of $A_0 = 0.00117$ and $A_1 = 0.00311$, and with a phase difference of $\phi_0 = 35°$.

IV. DISCUSSION

We have shown that the 109.3 s variation of G226–29 is a closely spaced triplet of pulsations with periods of 109.08684 s, 109.27929 s, and 109.47242 s. The pulsations are evenly spaced in frequency (not in period). The two side pulsations of the triplet have nearly equal fractional semiamplitudes of 0.0031, and the central pulsation has a lower amplitude of 0.0012. The ephemeris and precise parameters of the 109.3 s pulsations are given in Table 3.

Two of the other three ZZ Ceti stars whose light curves have been completely analyzed have groups of

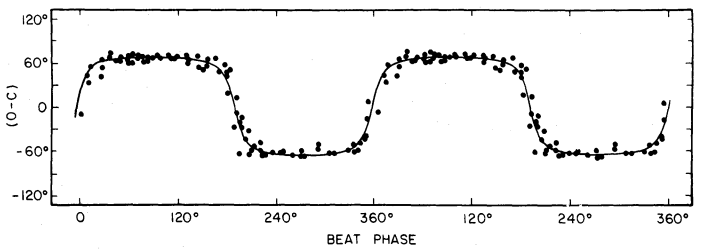

FIG. 8.—The $(O - C)$ diagram for the maxima of the 109.3 s variation. The dots are the same as in Fig. 6. The solid line is a plot of eq. (5) with semiamplitudes of $A_0 = 0.00117$ and $A_1 = 0.00311$, and with a phase difference of $\phi_0 = 35°$.

TABLE 3

SUMMARY OF RESULTS FOR G226–29

Differential Intensity Variation Formula
$I(t) = A_0 \cos\left[\frac{2\pi}{P_0}(t - T^0_{\max})\right] + A_1 \cos\left[\frac{2\pi}{P_1}(t - T^1_{\max})\right] + A_2 \cos\left[\frac{2\pi}{P_2}(t - T^2_{\max})\right]$
Periods
$P_0 = 109\overset{s}{.}27929 \pm 0\overset{s}{.}00002$
$P_1 = 109\overset{s}{.}08684 \pm 0\overset{s}{.}00002$
$P_2 = 109\overset{s}{.}47242 \pm 0\overset{s}{.}00002$
Fractional Semiamplitudes
$A_0 = 0.00117 \pm 0.00004$
$A_1 = 0.00305 \pm 0.00004$
$A_2 = 0.00317 \pm 0.00004$
HJED Times of Maxima
$T^0_{\max} = 4337.901243 \pm 0.000008$
$T^1_{\max} = 4337.902060 \pm 0.000003$
$T^2_{\max} = 4337.902144 \pm 0.000003$

pulsations similar to the 109.3 s triplet in G226–29: R548 has two close pairs of pulsations, and L19–2 has several triplets of pulsations (Stover *et al.* 1980; O'Donoghue 1981). The origin of the close groups in R548 and L19–2 is thought to be the removal of azimuthal degeneracy by slow rotation of the white dwarf. Nonradial pulsations with the same values of k and l, but different values of m, have the same pulsation periods if the white dwarf is not rotating and is otherwise spherically symmetric (we use the standard definitions of the pulsation indices k, l, and m). If, however, the white dwarf is rotating slowly, the coriolis force removes the azimuthal degeneracy, so that pulsations with different values of m have slightly different pulsation periods.

Slow rotation could also explain the origin of the 109.3 s triplet of pulsations in G226–29. The equatorial rotational velocity needed to produce the triplet is consistent with the low velocities normally observed in white dwarfs. Since the triplet pulsations are evenly spaced in frequency, and since the frequency separation is small, we can use linear theory to derive the velocity (Chlebowski 1978). In the linear theory, the relation between the frequency difference, Δf, and the velocity of rotation at the equator, V_r, is given by:

$$V_r = 2\pi R \Delta f (1 - C^I_{kl})^{-1}, \quad (6)$$

where R is the radius of the white dwarf, and C^I_{kl} is a coefficient that depends strongly on l, weakly on k, and is independent of m. As k increases, C^I_{kl} approaches the limit

$$C^I_{kl} = [l(l+1)]^{-1}, \quad (7)$$

but, according to Chlebowski, C^I_{kl} generally changes by less than 10% between $k = 1$ and $k = \infty$. Therefore, with little loss in accuracy, we can set

$$V_r = 2\pi R \Delta f \{1 - [l(l+1)]^{-1}\}. \quad (8)$$

We can use the detailed theoretical calculations by Winget (1981) to estimate the appropriate value for l. The g-mode pulsations of his white dwarf models with masses of 0.6 $M_\odot$, the observed mean mass of DA white dwarfs, have periods as short as 109 s only if l is greater than or equal to 3. Therefore, with $\Delta f = 1.61 \times 10^{-5}$ Hz, and adopting $R = 8.9 \times 10^3$ km and $l = 3$, we obtain a rotation velocity of $V_r = 1.0$ km s^{-1}. As values of l greater than 3 give nearly the same result, 1.0 km s^{-1} is the most likely equatorial rotational velocity of G226–29. Since the splitting by rotation of a pulsation mode with spherical index l gives rise to $(2l+1)$ separate pulsations, it is more natural to obtain three pulsations by choosing $l = 1$. For an $l = 1$ g-mode to have a period as short as 109 s, the white dwarf must have a mass greater than 1 $M_\odot$, that is, its mass must be much larger than the observed mean mass of DA white dwarfs. Assuming that the white dwarf mass is this large, and adopting $l = 1$, we obtain $V_r = 1.8$ km s^{-1}, so the rotational velocity still remains extremely low.

It is not possible to assign specific values of k, l, and m to the pulsations of G226–29 on purely observational grounds. In particular, our ignorance of the mass of G226–29 and of the inclination of its pulsation axis to the line of sight thwarts any attempt to assign specific values to l and m. Further progress in this direction appears to depend on more detailed—probably nonlinear—theoretical calculations.

The research reported in this paper was supported in part by NSF grant AST-8108691. We thank J. T. McGraw and G. Fontaine for communicating their results to us before publication, and H. Saio and D. Winget for their comments on our results.

REFERENCES

Bopp, B. W., Evans, D. S., Laing, J. D., and Deeming, T. J. 1970, *M.N.R.A.S.*, **147**, 355.
Chlebowski, T. 1978, *Acta Astr.*, **28**, 441.
Dolez, D., and Vauclair, G. 1981, *Astr. Ap.*, **102**, 375.
Giclas, H. L., Burnham, R., and Thomas, N. G. 1971, in *Lowell Proper Motion Survey* (Flagstaff, Az.: Lowell Observatory), p. 1.
Greenstein, J. L. 1982, *Ap. J.*, **261**, 1.

Kepler, S. O., Robinson, E. L., Nather, R. E., and McGraw, J. T. 1982, *Ap. J.*, **254**, 676.
McGraw, J. T. 1976, Ph.D. thesis, University of Texas at Austin.
Nather, R. E. 1973, *Vistas Astr.*, **15**, 91.
O'Donoghue, D. E. 1981, Ph.D. thesis, University of Cape Town.
Robinson, E. L. 1979, in *IAU Colloquium 53, White Dwarfs and Variable Degenerate Stars*, ed. H. M. Van Horn and V. Weidemann (Rochester, N.Y.: University of Rochester), p. 343.
Stover, R. J., Hesser, J. E., Lasker, B. M., Nather, R. E., and Robinson, E. L. 1980, *Ap. J.*, **240**, 865.
Winget, D. E. 1981, Ph.D. thesis, University of Rochester.
Winget, D. E., Van Horn, H. M., Tassoul, M., Hansen, C. J., Fontaine, G., and Carroll, B. W. 1982, *Ap. J.* (*Letters*), **252**, L65.

S. O. KEPLER, R. E. NATHER, and E. L. ROBINSON: Department of Astronomy, University of Texas at Austin, Austin, TX 78712